Cancer Cell
Article

Inhibition of Tumor Angiogenesis and Growth by a Small-Molecule Multi-FGF Receptor Blocker with Allosteric Properties

Françoise Bono,[1,15] Frederik De Smet,[2,3,15] Corentin Herbert,[1] Katrien De Bock,[2,3] Maria Georgiadou,[2,3] Pierre Fons,[1] Marc Tjwa,[2,3] Chantal Alcouffe,[1] Annelii Ny,[2,3] Marc Bianciotto,[1] Bart Jonckx,[2,3] Masahiro Murakami,[4] Anthony A. Lanahan,[4] Christof Michielsen,[5] David Sibrac,[1] Frédérique Dol-Gleizes,[1] Massimiliano Mazzone,[2,3] Serena Zacchigna,[2,3] Jean-Pascal Herault,[1] Christian Fischer,[2,3] Patrice Rigon,[1] Carmen Ruiz de Almodovar,[2,3] Filip Claes,[2,3] Isabelle Blanc,[1] Koen Poesen,[2,3] Jie Zhang,[5] Inmaculada Segura,[2,3] Geneviève Gueguen,[1] Marie-Françoise Bordes,[1] Diether Lambrechts,[2,3] Roselyne Broussy,[1] Marlies van de Wouwer,[2,3] Corinne Michaux,[1] Toru Shimada,[8] Isabelle Jean,[1] Silvia Blacher,[10] Agnès Noel,[10] Patrick Motte,[10] Eran Rom,[11] Jean-Marie Rakic,[9] Susumu Katsuma,[8] Paul Schaeffer,[1] Avner Yayon,[11] Ann Van Schepdael,[5] Harald Schwalbe,[12] Francesco Luigi Gervasio,[13] Geert Carmeliet,[6] Jef Rozensky,[7] Mieke Dewerchin,[2,3] Michael Simons,[4] Arthur Christopoulos,[14] Jean-Marc Herbert,[1,15] and Peter Carmeliet[2,3,15,*]

[1]Early to Candidate Department and Lead Generation and Candidate Realization Department, Sanofi, 31036 Toulouse, France
[2]Laboratory of Angiogenesis and Neurovascular Link, Vesalius Research Center, Department of Oncology, University of Leuven, Leuven, B-3000, Belgium
[3]Laboratory of Angiogenesis and Neurovascular link, Vesalius Research Center, VIB, Leuven, B-3000, Belgium
[4]Section of Cardiovascular Medicine, Department of Internal Medicine, Yale University School of Medicine, New Haven, CT 06520, USA
[5]Laboratory for Pharmaceutical Analysis, Pharmaceutical and Pharmacological Sciences
[6]Laboratory for Clinical and Experimental Endocrinology
[7]Medicinal Chemistry, Rega Instituut
KU Leuven, B-3000 Leuven, Belgium
[8]Department of Agricultural and Environmental Biology, School Agricultural and Life Sciences, University of Tokyo, 113-8657 Tokyo, Japan
[9]Department of Ophthalmology, University Hospital, CHU, Sart-Tilman, B-4000 Liège, Belgium
[10]Laboratory of Tumor and Development Biology, GIGA, University of Liège, B-4000 Liège, Belgium
[11]ProCore, Ltd., 10400 Nes Ziona, Israel
[12]Institute for Organic Chemistry and Chemical Biology, Center for Biomolecular Magnetic Resonance (BMRZ), University of Frankfurt, D-60438 Frankfurt, Germany
[13]Computational Biophysics Group, Spanish National Cancer Research Center (CNIO), E-28029 Madrid, Spain
[14]Drug Discovery Biology, Monash Institute of Pharmaceutical Sciences, Monash University, 3052 Victoria, Australia
[15]These authors contributed equally to this work
*Correspondence: peter.carmeliet@vib-kuleuven.be
http://dx.doi.org/10.1016/j.ccr.2013.02.019

SUMMARY

Receptor tyrosine kinases (RTK) are targets for anticancer drug development. To date, only RTK inhibitors that block orthosteric binding of ligands and substrates have been developed. Here, we report the pharmacologic characterization of the chemical SSR128129E (SSR), which inhibits fibroblast growth factor receptor (FGFR) signaling by binding to the extracellular FGFR domain without affecting orthosteric FGF binding. SSR exhibits allosteric properties, including probe dependence, signaling bias, and ceiling effects. Inhibition by SSR is highly conserved throughout the animal kingdom. Oral delivery of SSR inhibits arthritis and tumors that are relatively refractory to anti-vascular endothelial growth factor receptor-2 antibodies. Thus, orally active, extracellularly acting small-molecule modulators of RTKs with allosteric properties can be developed and may offer opportunities to improve anticancer treatment.

Significance

Receptor tyrosine kinases (RTK) represent key targets for anticancer drug development. Classic examples of RTK blockers include antibodies inhibiting orthosteric ligand binding, but small molecules that bind the extracellular domain of RTKs have traditionally not been considered because they are thought to be too small to competitively block binding of the much larger polypeptide ligands. We identified a small-molecule chemical compound, SSR128129E (SSR), which inhibits fibroblast growth factor receptor (FGFR) signaling through allosteric mechanisms after binding to the extracellular FGFR domain. Oral delivery of SSR inhibits tumor growth and amplifies anti-angiogenic drug therapy. These results offer incentives to develop orally active small-molecule RTK inhibitors with allosteric properties and opportunities for improved anticancer treatment.

INTRODUCTION

Cell-surface receptors represent key targets for drug development. Historically, drug discovery programs have been dominated by efforts to develop antagonists that compete for binding with endogenous ligands at orthosteric sites. Drugs that bind to allosteric sites, i.e., topographically distinct domains from those used by orthosteric ligands (if the target is a receptor) or substrates (if the target is an enzyme) that modulate a protein's activity, have been more difficult to identify. Recently, allosteric modulators have been identified for ligand-gated ion channels, G protein-coupled receptors (GPCRs), and kinases (Chahrour et al., 2012; Conn et al., 2009; Cox et al., 2011; Thaker et al., 2012).

Allosteric kinase inhibitors have been developed (Chahrour et al., 2012), but an extracellularly acting small-molecule allosteric inhibitor of receptor tyrosine kinases (RTKs) is not available. Yet, this receptor superfamily is of immense biomedical significance (Lemmon and Schlessinger, 2010). Furthermore, allosteric drugs offer therapeutic advantages over traditional orthosteric drugs, including greater safety and/or selectivity (Christopoulos, 2002). Most drugs targeting RTKs are antibodies against growth factor receptors that inhibit ligand binding or receptor dimerization or are small molecules inhibiting tyrosine kinase (TK) activity (Chung and Ferrara, 2011; Tvorogov et al., 2010). However, it is becoming increasingly clear that formation of receptor signaling complexes requires allosteric conformational changes in the extracellular domain to position the TK domains for signal transduction (Brozzo et al., 2012; Landgraf et al., 2010). Whether small molecules can inhibit or modulate RTK signaling by acting extracellularly remains unexplored.

Anti-angiogenic therapy would benefit from other RTK small-molecule inhibitors. Vascular endothelial growth factor (VEGF)-targeted agents prolong the survival of patients with cancer, but their success is restricted by refractoriness, escape, and in some models, increased metastasis (Bergers and Hanahan, 2008; Ebos and Kerbel, 2011). Combinatorial delivery of anti-angiogenic agents may help overcome these challenges (You et al., 2011).

Receptors for basic fibroblast growth factors (FGFs) are attractive drug candidates (Daniele et al., 2012; Itoh and Ornitz, 2011). FGF receptor (FGFR) signaling has been implicated in cancer, inflammation, and the escape of tumor vascularization from VEGF inhibitor treatment (Ahmad et al., 2012; Beenken and Mohammadi, 2009; Casanovas et al., 2005; Fischer et al., 2007; Malemud, 2007; Turner and Grose, 2010; Wesche et al., 2011). Nonetheless, the FGFR superfamily with its 18 ligands and four receptors has received little attention for drug development, partly because of redundancy (Beenken and Mohammadi, 2009). Selective TK inhibitors (TKIs) of FGFRs have not been clinically approved, and only broad-spectrum TKIs targeting primarily VEGF receptors (VEGFRs) and, less potently, FGFRs are available (Daniele et al., 2012; McDermott et al., 2005). This study characterizes an orally active, extracellularly acting small-molecule inhibitor of FGFRs.

RESULTS

Identification of SSR128129E

The compound SSR128129E ("SSR"; Figure 1A) was identified in a high-throughput screen, designed originally to discover orthosteric FGFR inhibitors. In this screen, we used a scintillation proximity assay (SPA) assay to identify chemicals blocking binding of ^{125}I-FGF2 to the extracellular domain of FGFR1-D1D2D3/Fc, the extracellular domain with 3 Ig-like domains D1-3 coupled to a Fc-fragment. A 10- to 100-fold molar excess of unlabeled FGF2 or anti-FGFR1 Fab (αFGFR1) inhibited ^{125}I-FGF2 binding completely, indicating that the assay identifies compounds inhibiting ligand binding via a competitive (orthosteric) mechanism (not shown). SSR emerged from this screen as a low-affinity antagonist (half maximal inhibitory concentration [IC_{50}]: 1.9 ± 1.4 μM).

Surprisingly, SSR was effective in the nanomolar range in cellular assays. Because FGF2 affects endothelial cells (ECs) in vitro, we used human umbilical venous endothelial cells (HUVECs) that express FGFR1 and lower levels of FGFR2 and FGFR4. SSR dose-dependently inhibited FGF2-induced EC proliferation (IC_{50}: 31 ± 1.6 nM; Figure 1B), migration (IC_{50}: 15.2 ± 4.5 nM; Figure 1C), and lamellipodia formation (Figure S1A available online). Thus, SSR inhibited EC responses with nanomolar potency, yet antagonized FGF binding only at micromolar levels. This puzzling result suggested that SSR was not acting as a classic orthosteric inhibitor and/or that its pharmacology was highly sensitive to the cellular environment and conformational properties of intact FGFR. We thus characterized its pharmacological properties.

SSR Is a Multi-FGFR Inhibitor

We investigated if SSR blocked the response to other FGFs, known to bind selectively to distinct FGFR subtypes. We therefore used cells from different species, expressing one or more FGFRs, and stimulated them with various FGF ligands. SSR inhibited responses mediated by FGFR1-4. For instance, SSR blocked EC migration in response to FGF1, a ligand of FGFR1 and FGFR4 (Figure 1C), and capillary tube formation in response to FGF19, a ligand of FGFR4 (Figure S1B). Proliferation and migration of the murine pancreatic Panc02 tumor cell line in response to FGF7 were also blocked by SSR (Figures 1D and 1E), showing that SSR inhibits FGFR subtypes of other species as well. Table 1 lists the nanomolar potency activities of SSR in blocking different FGFR subtypes in various cell lines used to analyze migratory, mitogenic, and other responses to FGF ligands. Notably, SSR inhibited FGFR paralogues in various species across the animal kingdom, including *Danio rerio* (zebrafish) (Figures S1C–S1F), *Drosophila melanogaster* (fruit fly) (Figures S1G-S1I), *Spodoptera frugiperda* (moth) (Figure S1J), and *Bombyx mori* (silkworm) (not shown).

The effect of SSR was not due to nonspecific toxicity because SSR (1 μM) failed to affect the mitogenic response to other stimuli of B9 myeloma cells or L6 myoblasts, which did not express FGFRs (not shown). Heparin (30 μg/ml) did not alter the inhibitory activity of SSR on the mitogenic or chemotactic response of FGFs (not shown).

SSR Inhibits FGFRs but Not Other Related RTKs

We then determined if SSR blocked the FGFR superfamily selectively. SSR did not affect responses to ligands activating structurally related RTKs (Figures 1E, 1F, and S1K). When FGF7 and VEGF were added together to test the migration of Panc02 tumor cells, SSR only blocked the response to

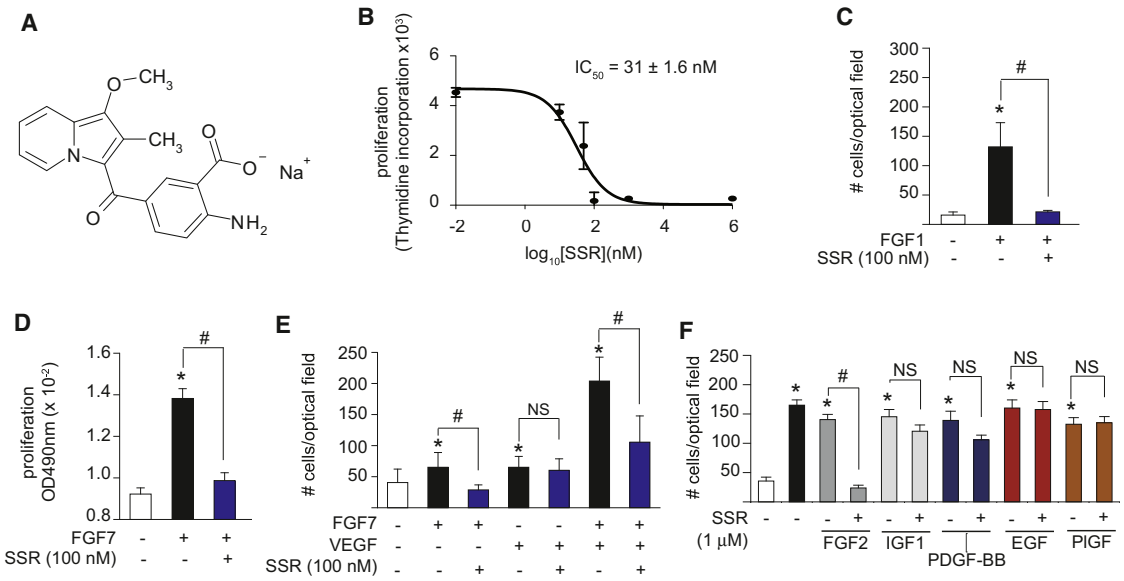

Figure 1. Activity and FGFR Specificity of SSR

(A) Chemical structure of SSR128129E (SSR).

(B) Effect of SSR on FGF2-induced EC proliferation.

(C) Effect of SSR (100 nM) on FGF1-driven EC migration (n = 3; *p < 0.05 versus control, #p < 0.05 versus FGF1 alone).

(D) Effect of SSR (100 nM) on FGF7-driven proliferation of Panc02 tumor cells (n = 3; *p < 0.05 versus control, #p < 0.05 versus FGF7 alone).

(E) Effect of SSR (100 nM) on migration of Panc02 tumor cells in response to single or combined stimulation with FGF7 and VEGF (n = 3; *p < 0.05 versus control, #p < 0.05 versus indicated condition).

(F) Effect of SSR (1 μM) on migration of ECs in response to different growth factors (n = 3; *p < 0.05 versus control, #p < 0.05 versus indicated condition). Data are presented as mean ± SEM.

See also Figure S1 and Tables S1 and S2.

FGF7 (Figure 1E). Similar results were obtained for the responses of ECs to VEGF plus FGF1 (not shown) or to VEGF plus FGF2 (Figure S1L), or of Panc02 cell responses to VEGF plus FGF7 (not shown). Genetic experiments in zebrafish to silence both *fgfr1* and *fgfr2* showed that SSR recapitulated quantitatively and qualitatively the phenotypic pharyngeal arch and cartilage defects, induced by combined silencing of *fgfr1* and *fgfr2*, underscoring that SSR is a multi-FGFR inhibitor (Figures S1M–S1T). SSR failed however to induce additional anomalies in zebrafish embryos lacking multiple FGFRs, showing that SSR specifically inhibited multiple FGFRs in an intact animal model without causing off-target effects (Figures S1U and S1V).

In contrast to a 10- or 100-fold molar excess of a neutralizing competitor or antibody, SSR failed to inhibit binding of VEGF, VEGF-B, placental growth factor, platelet-derived growth factor (PDGF)-BB, or PDGF-CC to their receptors, whose extracellular domains exhibit the highest homology to FGFRs. SSR also failed to inhibit phosphorylation of VEGFR2 or hepatocyte growth factor-receptor MET (Figures S1W and S1X; Table S1). SSR also did not alter receptor binding of interleukin-8, transforming growth factor-β, tumor necrosis factor-α, or epidermal growth factor, which are structurally more divergent from FGFs (Table S2). SSR also did not inhibit binding of >100 distinct ligands with related structural homology or entirely different chemical composition from FGFs, even when used at concentrations up to 10 μM (Table S2). Overall, SSR inhibited FGFR-driven responses while not affecting other related RTKs.

SSR Is Not a Potent Inhibitor of Orthosteric FGF Binding to FGFR

We then aimed at determining SSR's pharmacologic mechanism. The weak inhibition of the binding of ^{125}I-FGF2 to FGFR1-D1D2D3/Fc in the scintillation proximity assay (SPA) could be reconciled with a low-affinity orthosteric interaction or a low-affinity allosteric interaction exhibiting negative binding cooperativity (Christopoulos and Kenakin, 2002). However, such modest effects on the binding affinity of ^{125}I-FGF2 alone could not explain the greater potency of SSR in assays of cellular function. This would require a difference in binding affinity of SSR at the intact receptor expressed in a native environment and/or an allosteric effect on signal transduction (in addition to any negative cooperativity on orthosteric agonist binding).

To address these possibilities, we determined the potency of SSR as an inhibitor of the binding of ^{125}I-FGF2 to FGFRs when expressed in their native configuration in natural conditions on the EC surface. Under these conditions, the potency of SSR was reduced even more than in the SPA such that it was unable to inhibit ^{125}I-FGF2 binding to its receptors even at high micromolar concentrations (Figure 2A). In contrast, orthosteric inhibitors such as unlabeled FGF2, a neutralizing anti-FGF2 antibody or anti-FGFR1 (αFGFR1) blocked ^{125}I-FGF2 binding (Figure 2A). Thus, in this cellular binding assay, SSR did not act as a strong orthosteric inhibitor. Such contextual assay-dependent results are inconsistent with a simple competitive mechanism that relies on steric hindrance for an overlapping binding domain because the latter would yield consistent

Table 1. Effects of SSR on Cellular Responses to Different FGFRs

FGF Receptor	FGF Ligand	Cell Line	Cellular Assay	SSR Concentration Resulting in ≥50% Inhibition[a]
FGFR1IIIcα	FGF1	PAE-hFGFR1	Proliferation	100 nM[b]
	FGF2	PAE-hFGFR1	Proliferation	100 nM[b]
FGFR1IIIcβ	FGF1	HUVEC	Proliferation, migration	100 nM[b]
	FGF2	HUVEC	Proliferation, migration, survival	15–22 nM
	FGF4	HUVEC	Proliferation, migration	100 nM[b]
FGFR2IIIcα	FGF2	HEK-hFGFR2^{WT}	ERK activation	28 nM
FGFR2IIIb	FGF7	mPanc02	Proliferation, migration	100 nM[b]
FGFR3IIIcα	FGF1	hB9-myeloma	Proliferation	25 nM[b]
FGFR4IIIcα	FGF2	HUVEC	Proliferation, migration, survival	15–22 nM
	FGF19	HUVEC	Tube formation	10 nM[b]

PAE, porcine aortic endothelial cells.
[a]IC_{50} value of SSR (nM) determined by using various concentrations.
[b]Only two or three concentrations of SSR were tested without determining the precise IC_{50} value; in these cases, the indicated concentration already resulted in >50% inhibition.

inhibition of binding in all assays (as observed for unlabeled FGF2, αFGF2, and αFGFR1). Rather, these findings are characteristic of small-molecule allosteric modulators of other receptor classes that exert minimal effects on orthosteric ligand affinity (i.e., low negative cooperativity in the case of FGFR1-D1D2D3/Fc or neutral cooperativity in the case of intact FGFR) but have profound effects on orthosteric ligand signaling (Litschig et al., 1999). Indeed, the ability to mediate differential effects on the binding and function of orthosteric ligands in an assay-dependent manner is a typical feature of allosteric receptor modulators, referred to as "probe dependence" (Christopoulos and Kenakin, 2002; Litschig et al., 1999; Price et al., 2005).

Pharmacological Validation of an Allosteric Mechanism for SSR

SSR's inhibitory activity on FGFR signaling was not due to inhibition of dimerization of FGF receptors or ligands (Herbert et al., 2013). We thus used ECs and HEK293 cells stably expressing FGFR1 or FGFR3, respectively, to study whether SSR reduced FGFR phosphorylation in response to FGF1. FGFR immunoprecipitation, followed by blotting for phosphotyrosine, revealed that FGFR tyrosine phosphorylation in response to FGF1 was reduced by nanomolar SSR concentrations (Figures 2B and 2C). We thus explored if inhibition by SSR of FGFR-TK activity was consistent with an allosteric mechanism. At least four characteristic features of allosteric antagonists have been identified for other classes of cell-surface receptors, including: (1) the ability to act at a topographically distinct site away from orthosteric or substrate-binding sites; (2) the ability to display "probe dependence" (see above); (3) a saturability, or ceiling level, to the allosteric effect, above which no further antagonism is observed irrespective of ligand concentration; and (4) different degrees of inhibition depending on the signal pathway that is being modulated, a phenomenon referred to as "pathway bias" (Keov et al., 2011).

SSR Interacts with a Topographically Distinct Site

FGFR-TKIs, which competitively block binding of ATP to its orthosteric site in the TK domain, must cross the plasma membrane. High-performance liquid chromotography analysis indicated that lysates of cells treated with 10 μM SSR contained only background traces of SSR (Figure S2), indicating that SSR failed to cross the plasma membrane and did not accumulate at high levels intracellulary. Calculation by theoretical prediction of the octanol-water partition coefficient (theoretical $LogP_{OW}$: −2.018), a measure of the lipophilicity of the compound, also showed that SSR was preferentially distributed in a hydrophilic rather than hydrophobic milieu and thus unlikely to cross the plasma membrane.

Use of a recombinant FGFR1-TK domain revealed that even supraphysiologic concentrations of SSR failed to inhibit the TK activity in contrast to the FGFR-TK inhibitor SU5402 (Figure 2D). We also used B9 myeloma cells because they express a constitutively active FGFR3^{K650E} mutant, which stimulates cell proliferation in the absence of FGF. If SSR would be cell permeable and inhibit TK, then SSR should block the growth of FGFR3^{K650E} cells. In cells expressing wild-type FGFR3 (FGFR3^{WT}), FGF1 enhanced proliferation and this response was reduced by SSR (Figure 2E). As expected, FGF1 failed to further stimulate growth of FGFR3^{K650E} cells, while SSR was ineffective in reducing constitutively activated proliferation (Figure 2E). In contrast, SU5402 inhibited proliferation of both FGFR3^{WT} and FGFR3^{K650E} expressing B9 cells (Figure 2E).

Given that SSR indirectly blocked the FGFR-TK activity yet failed to cross the plasma membrane, we analyzed if SSR interacted with the extracellular domain of FGFR. We purified FGFR2-D2D3, a fragment of the extracellular domain of FGFR2 consisting of domain D2 and D3, and used mass spectrometry to determine if SSR bound to this fragment. Spectral analysis showed the predicted mass of FGFR2-D2D3 when measured in the absence of SSR (Mr = 24,493 Da) and revealed that the mass was augmented in the presence of a 10-fold molar excess of SSR by 322 Da, e.g., the molecular weight of SSR without Na^+ and H_2O (Figure 3A). This indicates that SSR binds with a stoichiometry of n = 1 to FGFR2-D2D3. SSR did not bind to FGFR2-D2L, consisting of D2 plus adjacent linker, indicating that SSR binds to D3 (Figure 3B). Because FGFR2-D2L contains the binding pocket for FGF, the lack of binding of SSR to FGFR2-D2L also supports our finding that SSR is unable to block orthosteric FGF binding. As negative control, no binding of SSR to FGF1 was detected (not shown), consistent with nuclear magnetic resonance studies (Herbert et al., 2013).

SSR Displays a Ceiling Level to Its Antagonism of FGFR Phosphorylation

SSR (100 nM) reduced tyrosine phosphorylation of FGFR1 and FGFR3 (see above). Remarkably, even a supramaximal

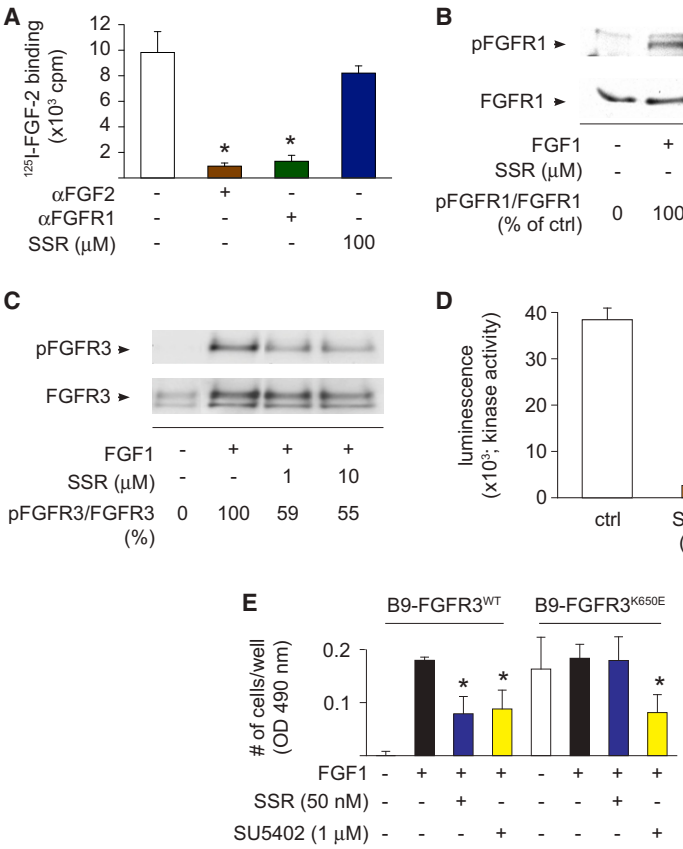

Figure 2. Mode of Action of SSR: Binding and Phosphorylation Assays

(A) Binding of ^{125}I-FGF2 to porcine aortic ECs (PAE) overexpressing FGFR1 with and without the orthosteric inhibitors anti-FGF2 (αFGF2) or anti-FGFR1 Fab (αFGFR1), or a 100-fold molar excess of SSR (100 μM). Data are corrected for residual background binding in the presence of 100-fold molar excess of unlabeled FGF2 ($n = 3$; $^*p < 0.05$).

(B) Immunoblotting with densitometric quantification of FGF1-induced tyrosine phosphorylation of FGFR1 in ECs in the absence or presence of SSR.

(C) Immunoblotting with densitometric quantification of FGF1-induced phosphorylation of wild-type FGFR3 in HEK293 cells in the absence or presence of SSR.

(D) Effect of SSR in a phosphorylation assay using the isolated kinase domain of FGFR1. The RTKI SU5402 was used as positive control ($n = 3$; $^*p < 0.05$).

(E) Effect of SSR on FGF1-induced proliferation of B9 myeloma cells expressing FGFR3^{WT} or the constitutively active FGFR3^{K650E} mutant. The RTKI SU5402 was used as positive control ($n = 3$; $^*p < 0.05$). Ctrl, control vehicle (DMSO). Quantitative data are presented as mean ± SEM.

See also Figure S2.

concentration of SSR (10 μM) did not completely eliminate FGFR but left a residual level of FGFR autophosphorylation (Figures 2B and 2C). This phenomenon cannot be reconciled with a competitive orthosteric mechanism and is another hallmark of allosteric interactions, namely a "ceiling level" to the actions of the allosteric modulator, above which no further pharmacologic effect is observed irrespective of modulator concentration (Conn et al., 2009; May et al., 2007). These findings suggest a limited negative cooperativity on FGFR signaling, in essence "tuning down" the degree of autophosphorylation to a new (lower) set-point. Similar data were obtained when analyzing tyrosine phosphorylation of FGFR1 and FGFR2 in HEK293 cells in response to FGF1 or FGF2 (not shown). We also analyzed the effect of increasing concentrations of SSR on the mitogenic response to different concentrations of FGF2, showing a shift to the right with increased sigmoidicity of the curve (Figure 3C), another hallmark of allostery (Christopoulos, 2002). This observation is comparable to effects observed for the allosteric antagonist 7-hydroxyimino-cyclopropan[b]chromen-1a-carboxylic acid ethyl ester of glutamate receptor 1 (Knoflach et al., 2001).

SSR Displays Pathway-Biased Antagonism of FGFR Signaling

Based on studies of allosteric modulators for other receptor classes, there is no a priori reason why conformational changes resulting from binding of the allosteric modulator should display equivalent degrees of allosteric modulation across different signaling pathways, if the allosteric interaction predominantly modulates orthosteric ligand efficacy rather than affinity (Leach et al., 2007)—a phenomenon referred to as "functional selectivity", "stimulus-trafficking", or "biased antagonism" (Urban et al., 2007). To assess if SSR induced biased antagonism, we generated a phosphomap of two major FGFR signaling pathways, i.e., FRS2-ERK1/2 and PLC-γ (Beenken and Mohammadi, 2009).

In FGFR2-expressing HEK293 cells (HEK-FGFR2), levels of phosphorylated FRS2 (pFRS2) and ERK1/2 (pERK1/2) were minimal in baseline and upregulated by FGF2 (Figures 3D and 3E). SSR and the pan-FGFR-TKI SU5402 inhibited phosphorylation of FRS2 and ERK1/2 (Figures 3D and 3E). However, unlike SU5402, SSR did not eliminate all FRS2 and ERK1/2 phosphorylation, in line with SSR's ceiling effect. Higher concentrations of FGF2 could not overcome the inhibition of ERK1/2 phosphorylation by SSR, further supporting the ceiling phenomenon (not shown). In the same cells, FGF2 elevated the levels of phosphorylated PLC-γ (pPLC-γ) (Figure 3F). In contrast to its inhibitory effect on FRS2 and ERK1/2, activation of PLC-γ was not blocked by SSR at the concentration (1 μM) that inhibited FRS2/ERK phosphorylation (Figure 3F). This induction of pPLC-γ was fully blocked by SU5402 (Figure 3F). Thus, SSR does not inhibit all FGFR signaling pathways indiscriminatively but selectively blocks particular signaling pathways, dependent on the cellular context. This biased antagonism of a RTK by a small molecule interacting with the extracellular domain can only be achieved via an allosteric mechanism. Collectively, our pharmacologic studies show that SSR exhibits all characteristic features of a small-molecule allosteric receptor inhibitor of FGF-driven cellular processes in vitro.

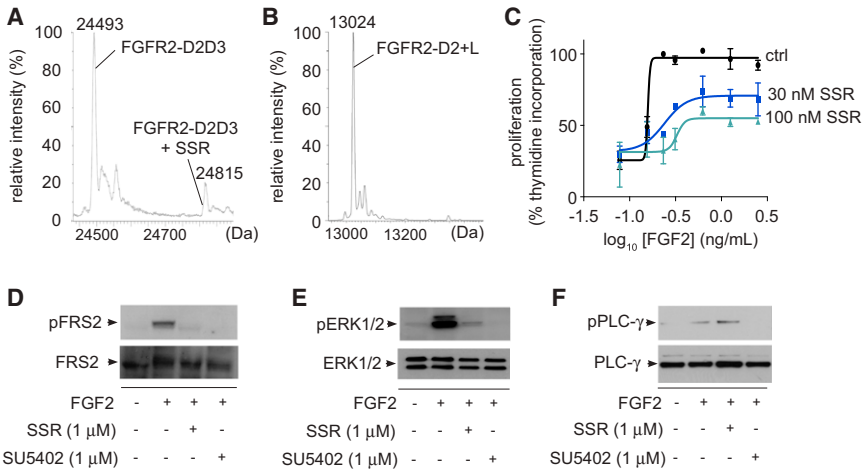

Figure 3. SSR-FGFR Binding Spectra and Effect on FGF-Signaling Pathways

(A and B) Spectra analysis of SSR binding to recombinant extracellular domain fragments of FGFR2. (A) The highest peak on the left corresponds to the expected molecular mass of the FGFR2-D2-3 fragment (24,493 Da); the peak on the right corresponds to the mass of FGFR2-D2-3 plus a single molecule of SSR (24,815 Da). (B) The highest peak corresponds to the expected molecular mass of FGFR2-D2L (13,024 Da).

(C) Effect of increasing SSR concentrations on the mitogenic response of ECs to increasing FGF2 concentrations. Ctrl, control vehicle (DMSO). Quantitative data are presented as mean ± SEM.

(D–F) Immunoblots for FGF2-induced tyrosine phosphorylation of FRS2 (D), ERK1/2 (E), or PLC-γ (F) in the absence or presence of SSR. The RTKI SU5402 was used as positive control.

SSR Inhibits Angiogenesis, Inflammation, and Bone Resorption in Arthritis

We then explored if SSR is capable of inhibiting inflammatory and malignant diseases, known as FGFR-driven processes (Malemud, 2007). Oral administration of SSR (30 mg/kg/day from day 3 onward; unless otherwise specified) reduced the number of limbs affected by redness, swelling, and deformity (3.6 ± 0.1 in controls versus 1.2 ± 0.1 after SSR; n = 10–14; $p < 0.001$). SSR reduced the severity of clinical symptoms (Figures 4A–4C) and slowed down its progression (day of maximal clinical score: 12.7 ± 0.3 days in controls versus 15.3 ± 0.8 days after SSR; n = 10; $p < 0.01$). Radiography revealed that SSR protected the mice against bone and joint damage (Figures 4D and 4E). SSR-treated mice also performed better in an exercise endurance test and ran longer on a treadmill (Figure 4F).

SSR reduced angiogenesis in the inflamed joints ($CD31^+$ vessels per optic field: 3.4 ± 1.6 in normal joints; 28.6 ± 4.2 in arthritic joints of controls versus 11.9 ± 4.6 in arthritic joints after SSR; n = 10–18; $p < 0.05$; Figures 4G and 4H). The antiangiogenic activity of SSR was confirmed in a matrigel model (hemoglobin content: 57 ± 10 mg/ml in control versus 12 ± 3 mg/ml in SSR mice; n = 5; $p < 0.05$). SSR attenuated synovial hyperplasia, inflammation, and pannus formation (Figures 4I, 4J,and 4M), and inhibited the infiltration of $CD45^+$ leukocytes ($CD45^+$ area, percentage of synovial area after 1 week: 14.5% ± 2.3% in controls versus 7.2% ± 1.5% after SSR; n = 5, $p < 0.05$) and osteoclast-mediated cartilage breakdown (safranin-O^+ area/μm: 12.1 ± 1.2 μm^2 in controls versus 16.5 ± 2.2 μm^2 after SSR; n = 18; $p < 0.05$; Figures 4K and 4L).

Oral SSR Delivery Delays Tumor Growth and Metastasis

We also analyzed if SSR inhibited tumor angiogenesis, growth, and metastasis using syngeneic and orthotopic tumor models and human xenograft tumor models. Oral delivery of SSR (30 mg/kg/day, from day 3) inhibited growth of orthotopic Panc02 tumors by 44% (Figures 5A, 5C, and 5E) and delayed growth of Lewis lung carcinoma (LLC) (end-stage tumor size and weight: 1,120 ± 120 mm^3 and 750 ± 80 mg in controls versus 720 ± 133 mm^3 and 430 ± 90 mg after SSR; n = 15; $p < 0.05$; Figure 5F). In murine 4T1 breast tumors, oral SSR (30 mg/kg/day, from day 5) reduced tumor size and weight by 53% and 40%, respectively (end-stage tumor size and weight: 2,050 ± 172 mm^3 and 840 ± 80 mg in controls versus 970 ± 127 mm^3 and 510 ± 80 mg after SSR; n = 15; $p < 0.001$; Figure 5G). In addition, SSR inhibited the growth of subcutaneous CT26 colon tumors by 34% (Figure 5H) and of the multidrug resistant MCF7/ADR breast cancer xenograft model by 40% (end-stage tumor volume: 250 ± 50 mm^3 in controls versus 152 ± 25 mm^3 after SSR; n = 15; $p < 0.01$). Tumor cells in these models expressed one or several FGFRs, while various FGF ligands were also detectable (not shown).

SSR reduced tumor invasiveness because the incidences of tumor invasion in healthy duodenum and of hemorrhagic ascites were lower in SSR-treated mice (75% and 58% of controls versus 15% and 8% of SSR-treated mice, respectively; n = 13; $p < 0.05$). Moreover, SSR inhibited metastasis of Panc02 tumor cells to peritoneal lymph nodes (metastatic nodules/mouse: 24 ± 2.6 in controls versus 8.3 ± 2.3 after SSR; n = 21; $p < 0.05$; Figures 5B and 5D). The reduced number of metastatic lymph nodes upon SSR treatment was not attributable to a reduction in tumor growth only because SSR decreased the metastatic index (metastatic nodes/gram tumor: 41 ± 3 for controls versus 30 ± 3 for SSR; n = 10; $p < 0.05$). In the LLC model, SSR reduced the number of pulmonary metastatic nodules by 43% after 3 weeks (lung metastases: 3.5 ± 0.3 in control versus 2.0 ± 0.3 after SSR; n = 15; $p < 0.05$). Similar results were obtained after orthotopic injection of 4T1 cells into the mammary gland (metastases per lung: 12.7 ± 1.4 in control versus 5.4 ± 0.4 after SSR; n = 15; $p < 0.001$). Altogether, SSR inhibited both the growth of primary tumors and metastasis.

SSR Enhances Tumor Growth Inhibition by Anti-VEGFR2

A substantial fraction of patients with cancer do not or only minimally respond to VEGFR inhibitor therapy (Ebos and Kerbel, 2011). Combinations of anti-angiogenic agents with complementary mechanisms may offer opportunities to overcome resistance. We therefore analyzed if SSR acts via a complementary mechanism to that of the anti-VEGFR2 antibody DC101 (αVEGFR2) (Witte et al., 1998) and if delivery of SSR enhanced the antitumor activity of αVEGFR2 using a model

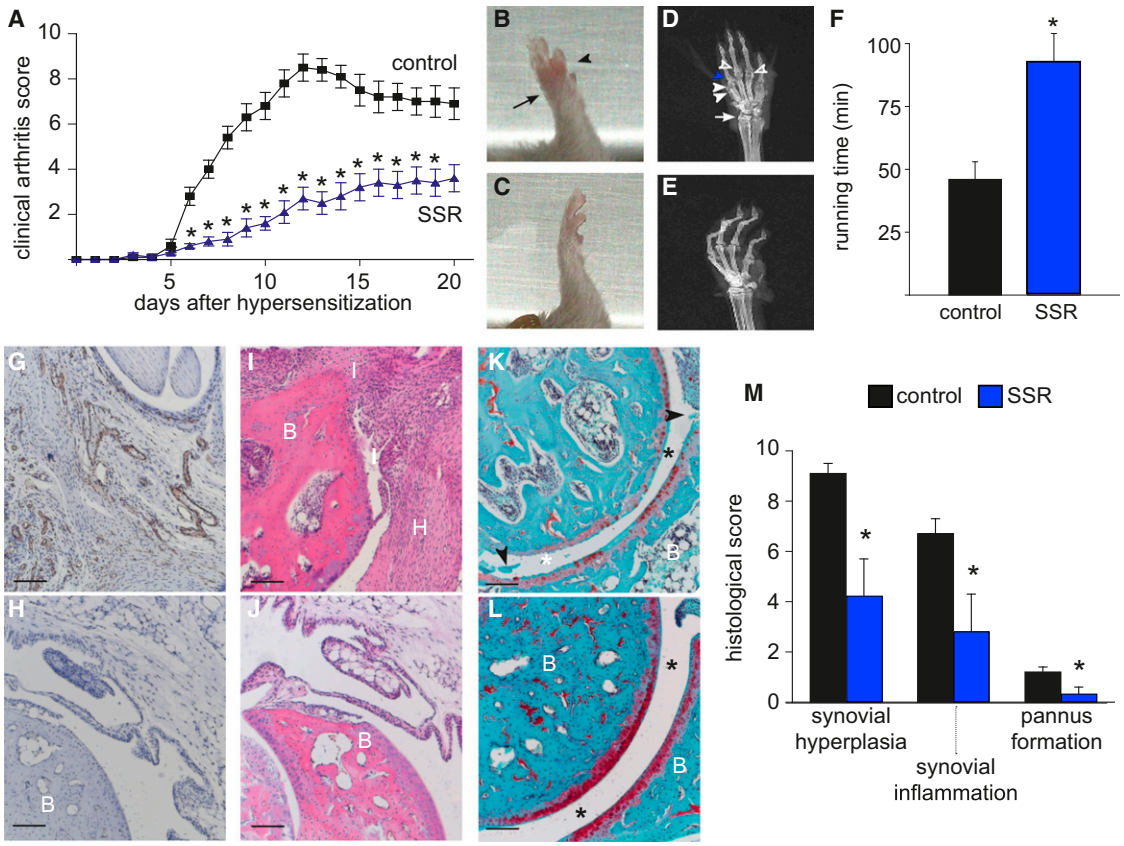

Figure 4. SSR Treatment of Inflammatory Joint Disease

(A) Clinical score of forelimbs and hindlimbs in arthritic mice treated with vehicle or SSR (30 mg/kg/day orally) (n = 10–14; $p < 0.001$ by repeated-measurement ANOVA; *$p < 0.05$ versus control at each time point).

(B and C) Micrographs of forelimb of mice treated with vehicle (B) or SSR (C). Black arrows and arrowheads point to swelling and redness of wrist or digits, respectively.

(D and E) X-ray images of forelimb of mice treated with vehicle (D) or SSR (E). White arrows: radiographic signs of aberrant bone formation; white arrowheads: osteolytic lesions, bone fractures, and bone remodeling; open arrowheads: loss or remodeling of joint space; blue arrowheads: joint fusion.

(F) Endurance treadmill exercise of control and SSR-treated arthritic mice at day 20 after hypersensitization (n = 7–12; *$p < 0.05$).

(G and H) Immunostaining of synovial blood vessels (CD31; brown) in control (G) and SSR-treated mice (H).

(I and J) Hematoxylin and eosin staining to visualize synovial hyperplasia and inflammation in control (I) and SSR-treated mice (J). B, bone; I, synovial inflammation; H, synovial hyperplasia.

(K and L) Safranin-O staining (red) of cartilage proteoglycans in control (K) and SSR-treated mice (L). Asterisks, the joint space; black arrowheads, presence of erosive bone fragment.

(M) Histologic score of synovial hyperplasia, inflammation, and pannus formation in control and SSR-treated mice (n = 5–9. *$p < 0.05$ versus control by Mann-Whitney). Scale bars: 100 μm (G–L). All quantitative data are presented as mean ± SEM.

that is more sensitive (Panc02 tumor) or more refractory (CT26 tumor) to VEGFR inhibitor therapy. In the Panc02 model, a low dose of αVEGFR2 (5 mg/kg; three times per week) inhibited tumor growth by ~40% (Figure 5E), which is comparable to the ~30% inhibition of tumor growth by a high dose of αVEGFR2 (50 mg/kg; three times per week; Figure 5H) in the CT26 model.

Mechanistically, both SSR and αVEGFR2 inhibited angiogenesis in Panc02 tumors ($CD31^+$ area: 5.0% ± 0.4% in control; 3.8% ± 0.3% after SSR; 2.9% ± 0.3% after DC101; n = 10; $p < 0.05$ for all treatments and for SSR versus αVEGFR2). SSR differed however from αVEGFR2 in its effect on macrophage infiltration. Indeed, in contrast to the lack of effect by αVEGFR2, SSR inhibited inflammatory cell infiltration in tumors (Figures 5I–5K). Similar findings were obtained for CT26 tumors (not shown). Thus, SSR inhibits tumor growth via mechanisms that differ from those utilized by αVEGFR2.

We therefore tested if a combination of SSR plus αVEGFR2 inhibited Panc02 tumor growth more extensively. SSR and αVEGFR2 each inhibited tumor growth by ~40%, while the combination treatment inhibited tumor growth by ~70% (Figure 5E). Similar results were obtained when analyzing the metastatic index (41% ± 3% for control; 30% ± 3% for SSR; 33% ± 3% for αVEGFR2 and 20% ± 1% for combination; n = 10; $p < 0.05$ for all treatments and for SSR versus αVEGFR2). When using the VEGFR inhibitor-refractory CT26 tumor model, the combination treatment inhibited tumor growth more than each monotherapy alone (Figure 5H). Thus, SSR acted via different mechanisms from those used by the VEGFR2 inhibitor,

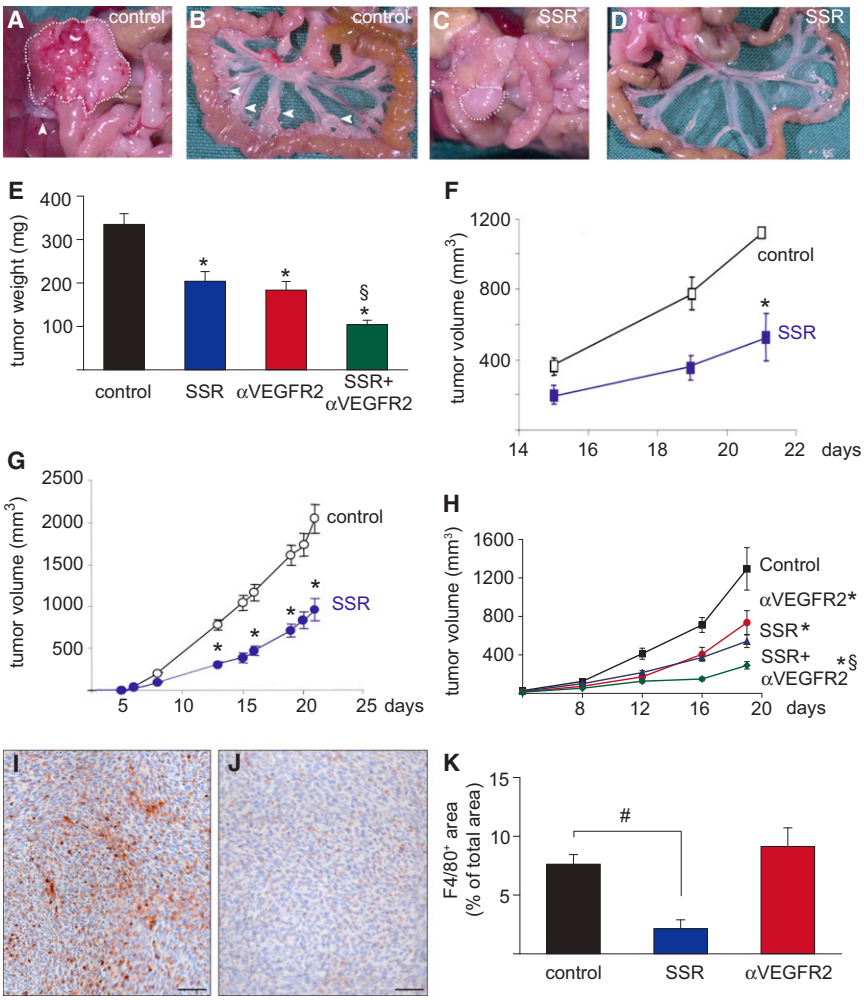

Figure 5. SSR Treatment of Malignant Disorders

(A–D) Effect of SSR (30 mg/kg/day orally) on orthotopic pancreatic Panc02 tumor growth. Representative images of the primary tumor (dashed line) in a control (A) or SSR-treated mouse (C). The white arrowhead in A denotes local infiltration of the primary tumor in the stomach and duodenum and a tumor-infiltrated celiac lymph node. Representative images show tumor-infiltrated mesenterial lymph nodes (white arrowheads) in control (B) and SSR-treated mice (D).

(E) Effect of single and combined treatment of orthotopically implanted Panc02 tumors with SSR (30 mg/kg/day) or αVEGFR2 (5 mg/kg; three times per week) on tumor weight as compared to vehicle-treated tumors (8–10 mice per group, n = 3; *$p < 0.05$ versus control; §$p < 0.05$ versus either monotherapy).

(F and G) Growth curve of subcutaneously implanted LLC tumors (F) and 4T1 breast tumors (G), upon treatment with vehicle (control) or SSR (30 mg/kg/day) (n = 3; *$p < 0.05$).

(H) Effect of single or combined treatment of subcutaneously implanted CT26 colon tumors with SSR (30 mg/kg/day) or αVEGFR2 (5 mg/kg; three times per week intraperitoneally) on tumor weight as compared to vehicle-treated tumors (8–10 mice per group, n = 3; *$p < 0.05$ versus control, §$p < 0.05$ versus either monotherapy).

(I–K) F4/80 immunostaining for macrophages in tumors of SSR-treated (J) versus control (I) mice. (K) shows quantification of tumor infiltration by F4/80$^+$ macrophages in SSR-treated compared to control or αVEGFR2-treated mice (n = 3; *$p < 0.05$). All quantitative data are presented as mean ± SEM. Scale bars: 100 μm (I, J).

inhibited growth of VEGFR inhibitor-refractory and -sensitive tumor models, and enhanced the antitumor activity of a VEGFR inhibitor.

Safety Profile

We assessed the safety profile of SSR by administering it to healthy mice during 3 weeks (30 mg/kg/day). A therapeutic dose of SSR did not cause vessel pruning (tracheal FITC$^+$ vessel area, percentage of total: 11.6% ± 1.1% in control versus 11.0% ± 0.6% after SSR; n = 6, p = NS), did not alter the mean arterial blood pressure (86 ± 3 mm Hg in controls versus 91 ± 4 mm Hg after SSR; n = 5; p = NS), and only minimally elevated plasma levels of the prothrombotic PAI-1 (1.0 ± 0.8 ng/ml in control versus 2.7 ± 0.6 ng/ml in SSR-treated mice; n = 5, p < 0.05). Hematologic parameters were normal after SSR, except for a minor anemia (red blood cells: 8.8 ± 0.1 10^6/ml in controls versus 8.3 ± 0.1 10^6/ml after SSR; n = 5; p < 0.05). SSR did also not significantly alter the body weight (21.2 ± 0.7 g in controls versus 19.3 ± 1.0 g after SSR; p = NS). In addition, daily treatment of Apo-E knockout mice with SSR for >6 months did not alter plasma cholesterol and triglyceride levels (not shown). Consistent with findings that SSR did not cross the blood-brain barrier, SSR did not impair neurologic performance (not shown).

DISCUSSION

We identified a small-molecule multi-FGFR inhibitor that does not block orthosteric ligand binding and does not act as a classic FGFR-TKI either. Instead, SSR negatively modulates selected FGFR signaling pathways with a pharmacologic profile characteristic of an allosteric mechanism.

Targeting the Fibroblast Growth Factor Receptor Superfamily by SSR

At least two reasons can explain the anti-inflammatory and anticancer activity of SSR. First, SSR is a multi-FGFR blocker with a broad action radius. This is necessary to overcome the substantial redundancy in this superfamily. Blocking a single FGFR with a monoclonal antibody may be beneficial for cancers arising from amplification or constitutive activation of a particular FGFR subtype (Ahmad et al., 2012; Qing et al., 2009; Turner and Grose, 2010). However, in most cancers, multiple FGFs are upregulated and various FGFR subtypes on tumor and stromal cells are activated (Turner and Grose, 2010). In such conditions, blocking a single FGFR may not suffice to yield therapeutic benefit. This may be particularly relevant for ECs, where FGFRs compensate for each other's loss. Indeed, mice,

zebrafish, or tadpoles lacking FGF/FGFRs do not exhibit vessel defects (Arman et al., 1998; Miller et al., 2000; Reifers et al., 2000; Zhou et al., 1998). Also, a genetic mouse study documented redundant roles of FGFRs in coronary vessel formation (Lavine et al., 2006). Hence, by blocking multiple FGFRs simultaneously, SSR not only has a broader action radius, but may also prevent compensatory rescue by other FGFR members.

A second explanation is that SSR inhibits multiple and diverse biologic processes that together synergistically fuel inflammation and tumorigenesis. FGFs induce multiple responses in nearly every cell type in the inflamed or malignant milieu (Malemud, 2007; Pietras et al., 2008). Consistent with findings that aberrant FGF-signaling stimulates tumor cell proliferation and migration, and induces epithelial-to-mesenchymal transition of tumor cells (Billottet et al., 2008; Strutz et al., 2002; Turner and Grose, 2010), SSR blocked FGF-driven proliferation and migration of tumor cells in vitro and slowed down tumor growth and reduced invasiveness and metastasis in vivo. FGFs can also activate FGFRs on ECs directly or stimulate angiogenesis indirectly by inducing the release of angiogenic factors from other cell types (Murakami and Simons, 2008; Presta et al., 2009). In accordance, SSR reduced FGF-driven EC proliferation, migration, and capillary tube formation in vitro and tumor angiogenesis in vivo. But FGFs also stimulate myeloid cells (Berardi et al., 1995), tumor-associated macrophages (Tsunoda et al., 2009), cancer-associated fibroblasts (Itoh, 2007; Kharitonenkov, 2009), and osteoclasts (Collin-Osdoby et al., 2002). Consistently, SSR reduced the accumulation of fibroblasts and myeloid cells in tumors and osteoclast-mediated breakdown of cartilage in arthritic joints. Thus, the anticancer/anti-inflammatory potential of SSR is likely due to a combined effect on many cell types. Because of the broad repertoire of cellular targets for FGFs, a multi-FGFR inhibitor like SSR might be expected to be instrumental in blocking a wider range of inflammatory and malignant diseases than analyzed in this study.

A Multi-Fibroblast Growth Factor Receptor Inhibitor with Allosteric Properties

Several lines of evidence indicate that SSR does not act as a classic orthosteric inhibitor of FGF binding because it failed to competitively antagonize binding of FGF2 to FGFRs in a natural context. SSR also did not act as a classic RTK inhibitor because it exhibits a hydrophilic partition coefficient, did not cross the plasma membrane, and failed to block the kinase activity of FGFR TK domains and a constitutively active TK of FGFR3 in cells.

Instead, SSR exhibits pharmacologic characterstics of an allosteric modulator. Mass spectrometry showed that SSR bound to a site in extracellular D2 or D3 of FGFR2 and failed to bind to a fragment containing D2 and its adjacent linker, implying that SSR likely binds a site in D3. Additional biophysical studies support binding of SSR to D3 (Herbert et al., 2013). Because D2 and its adjacent linker are critical for orthosteric FGF binding, the absence of binding of SSR to this fragment provides circumstantial evidence that SSR does not interfere with orthosteric FGF binding. It would be otherwise puzzling to explain how a small molecule like SSR is capable of inhibiting the responses of FGFRs to multiple FGF ligands via steric hindrance of the orthosteric FGFR pocket, given that FGFs are large polypeptides that utilize multiple epitopes for interaction with their receptors (Beenken and Mohammadi, 2009).

Instead, an allosteric mechanism more likely explains how a small molecule can perturb binding and signaling of a much larger ligand, and our pharmacologic analyses indicate that SSR displays typical pharmacologic hallmarks of an allosteric modulator. For instance, a characteristic of SSR's allosteric interactions was the phenomenon of "probe dependence" i.e., variations in magnitude and direction of an allosteric interaction depending on the nature of the orthosteric ligand-receptor complex with which the modulator is interacting (Christopoulos and Kenakin, 2002; Litschig et al., 1999; May et al., 2007; Price et al., 2005). Binding cooperativity was negative in the SPA with a predimerized Fc-coupled extracellular domain of FGFR2, while it was neutral in the cellular binding assays to a naturally folded and signaling-capable FGFR2. An additional key allosteric feature was the ceiling level (limit) to the degree of inhibition of FGFR tyrosine phosphorylation and ERK1/2 phosphorylation by SSR at high concentrations, as observed for other allosteric modulators (May et al., 2007). SSR also showed a bias toward antagonizing selected FGFR signaling pathways to the relative exclusion of others. This phenomenon cannot be explained by a competitive orthosteric mechanism; if SSR's mode of antagonism was based on steric hindrance of FGF ligands, then all pathways should be blocked nondiscriminatively to the same extent. Overall, rather than acting as an allosteric "affinity modulator", SSR acts as an allosteric "efficacy modulator" (Conn et al., 2009). The finding that SSR inhibits FGFR orthologues and paralogues throughout the animal kingdom suggests that it binds to a conserved allosteric site in the FGFRs. In the accompanying manuscript (Herbert et al., 2013), we characterized the molecular mechanisms of the allosteric properties of the SSR compound.

Possible Implications

From a therapeutic perspective, our studies highlight opportunities for multi-FGFR inhibitors in arthritis and cancer. An intriguing question is if SSR might be useful as an anticancer agent for the treatment of VEGFR-inhibitor-resistant tumors, given that FGFs belong to a class of "rescue" angiogenic factors, when tumor-bearing mice or patients are treated with VEGF inhibitors (Ebos and Kerbel, 2011).

Most anticancer drugs are administered at maximal tolerable dose to block the target's activity as maximally as possible. However, such a strategy may cause adverse effects. Preclinical studies report that high doses of orthosteric VEGF blockers, causing high-grade inhibition of VEGF signaling, induce undesired erythrocytosis (Tam et al., 2006) and fuel metastasis in preclinical models in particular (Ebos and Kerbel, 2011; You et al., 2011). In contrast, irrespective of its dose, an allosteric inhibitor has a ceiling effect and cannot completely wipe out RTK signaling, thus leaving a residual level of baseline signaling that may suffice to ensure cellular homeostasis and prevent evocation of undesired responses. Studies of GPCRs and ion channels show that an allosteric mode of drug-receptor interaction offers opportunities for fine-tuning biologic responses in a manner that is not attainable via classic orthosteric mechanisms (Conn et al., 2009). Finally, from a drug development perspective, our data offer an incentive to develop orally

deliverable small-molecule allosteric RTK inhibitors that bind to an extracellular domain.

EXPERIMENTAL PROCEDURES

Compound Characteristics

Chemical features of SSR128129E are described in the Supplemental Experimental Procedures. Upon oral treatment of mice with 30 mg/kg, a maximal plasma concentration (C_{max}) of 15.2 ± 0.5 mg/l was achieved at 15 min after treatment. The half-life ($T_{1/2}$) was 18.4 hr and the area under the curve at 0–48 hr (AUC_{0-48hr}) was 138.5 mg/hr/l. When rats were treated orally with 10 mg/kg, the C_{max} was 5.3 mg/l, the $T_{1/2}$ was 5.6 hr, the AUC_{0-24h} was 28.3 mg/hr/l, and the V_{ss} was 1.7 l/kg, and 64% of administered SSR was available in the plasma. SSR was not detectable in the cerebrospinal fluid, showing that it was unable to pass through the blood-brain barrier while it did accumulate in peripheral organs (tissue/plasma ratio for liver is 2–3; for brain, 0.01).

Binding Experiments

SPA were performed using FGFR1IIIcβ/Fc and ^{125}I-FGF2, and cellular binding assays by using ^{125}I-FGF2 or ELISA. Binding assays listed in Table S1 were performed by CEREP (Poitiers, France).

Cell Proliferation and Migration Assays

HUVECs, freshly isolated from different donors and used between passage two and five, were cultured in M199 medium (Invitrogen, Life Technologies, Ghent, Belgium) supplemented with 20% fetal bovine serum (FBS), 2 mM L-glutamine, 30 mg/l endothelial cell growth factor supplements (EGCS), 10 units/ml heparin, and penicillin/streptomycin (Lonza, Braine l'Alleud, Belgium). For proliferation, ECs were starved overnight in growth factor-depleted M199 medium containing 2% FBS and stimulated for 24 hr with 10 ng/ml bFGF with SSR or DMSO. Proliferation was assessed the last 2 hr by incubation with 1 μCi/ml [^{3}H]thymidine (Perkin Elmer, Zaventem, Belgium). Proliferation of porcine aortic endothelial (PAE) and tumor cell lines was measured using the CellTiter 96 Aqueous One Solution Cell Proliferation Assay (Promega, Madison, Wisconsin, USA), and cell migration was assessed by a modified Boyden chamber assay, as detailed in the Supplemental Experimental Procedures. Lamellipodia formation and capillary tube formation was assessed as described (Mazzone et al., 2009). Each assay was performed in triplicate and repeated at least three times. B9-FGFR3^{WT} and B9-FGFR3^{K650E} were obtained from S. Trudel (Toronto, ON, Canada).

Fibroblast Growth Factor Receptor Phosphorylation and Tyrosine Kinase Assay

Rat fat-pad endothelial (RFPE) cells expressing FGFR1IIIcα-hemaglutinin, Sf-9 cells expressing His-tagged *Bmbtl*, and HEK293 cells expressing FGFR1IIIca, FGFR2IIIca, or FGFR1IIIcβ were stimulated with FGFs in the presence or absence of SSR. HA-tagged proteins or FGFRs were immunoprecipitated with an anti-HA-antibody and immunoblotted with HRP-conjugated anti-PY or HRP-conjugated anti-HA. Kinase activity measurements of the recombinant catalytic domain of FGFR1 (Sigma-Aldrich, Bornem, Belgium) were done using the ADP-Glo Kinase Assay (Promega, Madison, Wisconsin, USA).

Mass Spectrometry

Mass spectra using purified FGFR2$^{\partial 23}$ and FGFR2$^{\partial 2+L}$ were acquired on a quadrupole orthogonal acceleration time-of-flight mass spectrometer equipped with standard electrospray source. Sample solutions were prepared in acetonitrile/water (1/1 v/v) containing 1% (v/v) acetic acid. The electrospray capillary voltage was 3,000 V and cone voltage 30 V. Nitrogen gas was used for nebulization and desolvation. Spectra were deconvoluted using the MaxEnt algorithm.

Animal Experiments

All procedures and care of animals were approved by the Institutional Animal Care and Research Advisory Committee (KU Leuven, Belgium) and Use Committees of Sanofi-Synthelabo Recherche (France). All animal experiments were performed in accordance with the institutional and national guidelines and regulations and are described extensively in the Supplemental Experimental Procedures.

Statistics

All data represent the mean ± SEM of the indicated number of experiments. We used SPSS v.11.0 for statistical calculations. IC_{50} values were calculated using Prism v4.0b. Statistical significance was calculated by the indicated test, considering $p < 0.05$ as statistically significant.

A more extended version of the materials and methods can be found in the Supplemental Experimental Procedures.

SUPPLEMENTAL INFORMATION

Supplemental Information includes two figures, two tables, and Supplemental Experimental Procedures and can be found with this article online at http://dx.doi.org/10.1016/j.ccr.2013.02.019.

ACKNOWLEDGMENTS

H.S. is supported by the DFG-Cluster of Excellence (EXC115) and by the state of Hesse. M.S. and M.M. are supported by NIH grant HL53793. A.C. is a Senior Research Fellow of the National Health and Medical Research Council of Australia. This work is supported, in part, by grants G.0567.05, G.0405.05, G.0405.06, and G.0789.11 from the FWO, Belgium; GOA/2006/11 from the Concerted Research Activities, Belgium; grant #LSHG-CT-2004-503573 from the EU 6th Framework Program; the Belgian Science Policy (IAP #P5-02 and IAP #P6-30); Leducq Network of Excellence; and long-term structural Methusalem funding by the Flemish Government to P.C. The authors are grateful to M. Krasnow for providing *Btl*-EGFP fruitflies, S. Trudel and Zhihua Li for providing B9 myeloma cell lines, and Lena Claesson-Welsh for providing PAE-FGFR1 cells.

F.B., C.H., C.A., M.B., D.S., F.D.-G., J.P.H., P.R., I.B., G.G., M.F.B., R.B., C.M., I.J., P.S., and J.M.H. are employees of Sanofi-Aventis, Toulouse, France. This work was sponsored in part by a grant from Sanofi-Aventis (to P.C.). P.C., C.H., and F.D. are inventors on the international patent application "extracellular allosteric inhibitor binding domain from a tyrosine kinase receptor" with publication number WO2011/001413 and its national counterparts.

Received: March 17, 2012
Revised: July 24, 2012
Accepted: February 19, 2013
Published: April 15, 2013

REFERENCES

Ahmad, I., Iwata, T., and Leung, H.Y. (2012). Mechanisms of FGFR-mediated carcinogenesis. Biochim. Biophys. Acta *1823*, 850–860.

Arman, E., Haffner-Krausz, R., Chen, Y., Heath, J.K., and Lonai, P. (1998). Targeted disruption of fibroblast growth factor (FGF) receptor 2 suggests a role for FGF signaling in pregastrulation mammalian development. Proc. Natl. Acad. Sci. USA *95*, 5082–5087.

Beenken, A., and Mohammadi, M. (2009). The FGF family: biology, pathophysiology and therapy. Nat. Rev. Drug Discov. *8*, 235–253.

Berardi, A.C., Wang, A., Abraham, J., and Scadden, D.T. (1995). Basic fibroblast growth factor mediates its effects on committed myeloid progenitors by direct action and has no effect on hematopoietic stem cells. Blood *86*, 2123–2129.

Bergers, G., and Hanahan, D. (2008). Modes of resistance to anti-angiogenic therapy. Nat. Rev. Cancer *8*, 592–603.

Billottet, C., Tuefferd, M., Gentien, D., Rapinat, A., Thiery, J.P., Broët, P., and Jouanneau, J. (2008). Modulation of several waves of gene expression during FGF-1 induced epithelial-mesenchymal transition of carcinoma cells. J. Cell. Biochem. *104*, 826–839.

Brozzo, M.S., Bjelić, S., Kisko, K., Schleier, T., Leppänen, V.M., Alitalo, K., Winkler, F.K., and Ballmer-Hofer, K. (2012). Thermodynamic and structural

description of allosterically regulated VEGFR-2 dimerization. Blood *119*, 1781–1788.

Casanovas, O., Hicklin, D.J., Bergers, G., and Hanahan, D. (2005). Drug resistance by evasion of antiangiogenic targeting of VEGF signaling in late-stage pancreatic islet tumors. Cancer Cell *8*, 299–309.

Chahrour, O., Cairns, D., and Omran, Z. (2012). Small molecule kinase inhibitors as anti-cancer therapeutics. Mini Rev. Med. Chem. *12*, 399–411.

Christopoulos, A. (2002). Allosteric binding sites on cell-surface receptors: novel targets for drug discovery. Nat. Rev. Drug Discov. *1*, 198–210.

Christopoulos, A., and Kenakin, T. (2002). G protein-coupled receptor allosterism and complexing. Pharmacol. Rev. *54*, 323–374.

Chung, A.S., and Ferrara, N. (2011). Developmental and pathological angiogenesis. Annu. Rev. Cell Dev. Biol. *27*, 563–584.

Collin-Osdoby, P., Rothe, L., Bekker, S., Anderson, F., Huang, Y., and Osdoby, P. (2002). Basic fibroblast growth factor stimulates osteoclast recruitment, development, and bone pit resorption in association with angiogenesis in vivo on the chick chorioallantoic membrane and activates isolated avian osteoclast resorption in vitro. J. Bone Miner. Res. *17*, 1859–1871.

Conn, P.J., Christopoulos, A., and Lindsley, C.W. (2009). Allosteric modulators of GPCRs: a novel approach for the treatment of CNS disorders. Nat. Rev. Drug Discov. *8*, 41–54.

Cox, K.J., Shomin, C.D., and Ghosh, I. (2011). Tinkering outside the kinase ATP box: allosteric (type IV) and bivalent (type V) inhibitors of protein kinases. Fut Med. Chem. *3*, 29–43.

Daniele, G., Corral, J., Molife, L.R., and de Bono, J.S. (2012). FGF receptor inhibitors: role in cancer therapy. Curr. Oncol. Rep. *14*, 111–119.

Ebos, J.M., and Kerbel, R.S. (2011). Antiangiogenic therapy: impact on invasion, disease progression, and metastasis. Nature reviews. Clin. Oncol. *8*, 210–221.

Fischer, C., Jonckx, B., Mazzone, M., Zacchigna, S., Loges, S., Pattarini, L., Chorianopoulos, E., Liesenborghs, L., Koch, M., De Mol, M., et al. (2007). Anti-PlGF inhibits growth of VEGF(R)-inhibitor-resistant tumors without affecting healthy vessels. Cell *131*, 463–475.

Herbert, C., Schieborr, U., Saxena, K., Juraszek, J., De Smet, F., Alcouffe, C., Bianciotto, M., Saladino, G., Sibrac, D., Kudlinzki, D., et al. (2013). Molecular mode of action of SSR128129E, a small molecule allosteric inhibitor of FGF receptor signaling. Cancer Cell. *23*, this issue, 489–501.

Itoh, N. (2007). The Fgf families in humans, mice, and zebrafish: their evolutional processes and roles in development, metabolism, and disease. Biol. Pharm. Bull. *30*, 1819–1825.

Itoh, N., and Ornitz, D.M. (2011). Fibroblast growth factors: from molecular evolution to roles in development, metabolism and disease. J. Biochem. *149*, 121–130.

Keov, P., Sexton, P.M., and Christopoulos, A. (2011). Allosteric modulation of G protein-coupled receptors: a pharmacological perspective. Neuropharmacology *60*, 24–35.

Kharitonenkov, A. (2009). FGFs and metabolism. Curr. Opin. Pharmacol. *9*, 805–810.

Knoflach, F., Mutel, V., Jolidon, S., Kew, J.N., Malherbe, P., Vieira, E., Wichmann, J., and Kemp, J.A. (2001). Positive allosteric modulators of metabotropic glutamate one receptor: characterization, mechanism of action, and binding site. Proc. Natl. Acad. Sci. USA *98*, 13402–13407.

Landgraf, K.E., Santell, L., Billeci, K.L., Quan, C., Young, J.C., Maun, H.R., Kirchhofer, D., and Lazarus, R.A. (2010). Allosteric peptide activators of prohepatocyte growth factor stimulate Met signaling. J. Biol. Chem. *285*, 40362–40372.

Lavine, K.J., White, A.C., Park, C., Smith, C.S., Choi, K., Long, F., Hui, C.C., and Ornitz, D.M. (2006). Fibroblast growth factor signals regulate a wave of Hedgehog activation that is essential for coronary vascular development. Genes Dev. *20*, 1651–1666.

Leach, K., Sexton, P.M., and Christopoulos, A. (2007). Allosteric GPCR modulators: taking advantage of permissive receptor pharmacology. Trends Pharmacol. Sci. *28*, 382–389.

Lemmon, M.A., and Schlessinger, J. (2010). Cell signaling by receptor tyrosine kinases. Cell *141*, 1117–1134.

Litschig, S., Gasparini, F., Rueegg, D., Stoehr, N., Flor, P.J., Vranesic, I., Prézeau, L., Pin, J.P., Thomsen, C., and Kuhn, R. (1999). CPCCOEt, a noncompetitive metabotropic glutamate receptor 1 antagonist, inhibits receptor signaling without affecting glutamate binding. Mol. Pharmacol. *55*, 453–461.

Malemud, C.J. (2007). Growth hormone, VEGF and FGF: involvement in rheumatoid arthritis. Clin. Chim. Acta *375*, 10–19.

May, L.T., Leach, K., Sexton, P.M., and Christopoulos, A. (2007). Allosteric modulation of G protein-coupled receptors. Annu. Rev. Pharmacol. Toxicol. *47*, 1–51.

Mazzone, M., Dettori, D., Leite de Oliveira, R., Loges, S., Schmidt, T., Jonckx, B., Tian, Y.M., Lanahan, A.A., Pollard, P., Ruiz de Almodovar, C., et al. (2009). Heterozygous deficiency of PHD2 restores tumor oxygenation and inhibits metastasis via endothelial normalization. Cell *136*, 839–851.

McDermott, L.A., Simcox, M., Higgins, B., Nevins, T., Kolinsky, K., Smith, M., Yang, H., Li, J.K., Chen, Y., Ke, J., et al. (2005). RO4383596, an orally active KDR, FGFR, and PDGFR inhibitor: synthesis and biological evaluation. Bioorg. Med. Chem. *13*, 4835–4841.

Miller, D.L., Ortega, S., Bashayan, O., Basch, R., and Basilico, C. (2000). Compensation by fibroblast growth factor 1 (FGF1) does not account for the mild phenotypic defects observed in FGF2 null mice. Mol. Cell. Biol. *20*, 2260–2268.

Murakami, M., and Simons, M. (2008). Fibroblast growth factor regulation of neovascularization. Curr. Opin. Hematol. *15*, 215–220.

Pietras, K., Pahler, J., Bergers, G., and Hanahan, D. (2008). Functions of paracrine PDGF signaling in the proangiogenic tumor stroma revealed by pharmacological targeting. PLoS Med. *5*, e19.

Presta, M., Andrés, G., Leali, D., Dell'Era, P., and Ronca, R. (2009). Inflammatory cells and chemokines sustain FGF2-induced angiogenesis. Eur. Cytokine Netw. *20*, 39–50.

Price, M.R., Baillie, G.L., Thomas, A., Stevenson, L.A., Easson, M., Goodwin, R., McLean, A., McIntosh, L., Goodwin, G., Walker, G., et al. (2005). Allosteric modulation of the cannabinoid CB1 receptor. Mol. Pharmacol. *68*, 1484–1495.

Qing, J., Du, X., Chen, Y., Chan, P., Li, H., Wu, P., Marsters, S., Stawicki, S., Tien, J., Totpal, K., et al. (2009). Antibody-based targeting of FGFR3 in bladder carcinoma and t(4;14)-positive multiple myeloma in mice. J. Clin. Invest. *119*, 1216–1229.

Reifers, F., Walsh, E.C., Léger, S., Stainier, D.Y., and Brand, M. (2000). Induction and differentiation of the zebrafish heart requires fibroblast growth factor 8 (fgf8/acerebellar). Development *127*, 225–235.

Strutz, F., Zeisberg, M., Ziyadeh, F.N., Yang, C.Q., Kalluri, R., Müller, G.A., and Neilson, E.G. (2002). Role of basic fibroblast growth factor-2 in epithelial-mesenchymal transformation. Kidney Int. *61*, 1714–1728.

Tam, B.Y., Wei, K., Rudge, J.S., Hoffman, J., Holash, J., Park, S.K., Yuan, J., Hefner, C., Chartier, C., Lee, J.S., et al. (2006). VEGF modulates erythropoiesis through regulation of adult hepatic erythropoietin synthesis. Nat. Med. *12*, 793–800.

Thaker, T.M., Kaya, A.I., Preininger, A.M., Hamm, H.E., and Iverson, T.M. (2012). Allosteric mechanisms of G protein-Coupled Receptor signaling: a structural perspective. Methods Mol. Biol. *796*, 133–174.

Tsunoda, S., Sakurai, H., Saito, Y., Ueno, Y., Koizumi, K., and Saiki, I. (2009). Massive T-lymphocyte infiltration into the host stroma is essential for fibroblast growth factor-2-promoted growth and metastasis of mammary tumors via neovascular stability. Am. J. Pathol. *174*, 671–683.

Turner, N., and Grose, R. (2010). Fibroblast growth factor signalling: from development to cancer. Nat. Rev. Cancer *10*, 116–129.

Tvorogov, D., Anisimov, A., Zheng, W., Leppänen, V.M., Tammela, T., Laurinavicius, S., Holnthoner, W., Heloterä, H., Holopainen, T., Jeltsch, M., et al. (2010). Effective suppression of vascular network formation by combination of antibodies blocking VEGFR ligand binding and receptor dimerization. Cancer Cell *18*, 630–640.

Urban, J.D., Clarke, W.P., von Zastrow, M., Nichols, D.E., Kobilka, B., Weinstein, H., Javitch, J.A., Roth, B.L., Christopoulos, A., Sexton, P.M., et al. (2007). Functional selectivity and classical concepts of quantitative pharmacology. J. Pharmacol. Exp. Ther. *320*, 1–13.

Wesche, J., Haglund, K., and Haugsten, E.M. (2011). Fibroblast growth factors and their receptors in cancer. Biochem. J. *437*, 199–213.

Witte, L., Hicklin, D.J., Zhu, Z., Pytowski, B., Kotanides, H., Rockwell, P., and Böhlen, P. (1998). Monoclonal antibodies targeting the VEGF receptor-2 (Flk1/KDR) as an anti-angiogenic therapeutic strategy. Cancer Metastasis Rev. *17*, 155–161.

You, W.K., Sennino, B., Williamson, C.W., Falcón, B., Hashizume, H., Yao, L.C., Aftab, D.T., and McDonald, D.M. (2011). VEGF and c-Met blockade amplify angiogenesis inhibition in pancreatic islet cancer. Cancer Res. *71*, 4758–4768.

Zhou, M., Sutliff, R.L., Paul, R.J., Lorenz, J.N., Hoying, J.B., Haudenschild, C.C., Yin, M., Coffin, J.D., Kong, L., Kranias, E.G., et al. (1998). Fibroblast growth factor 2 control of vascular tone. Nat. Med. *4*, 201–207.